*OG.2.1.16*

# TeV-Characteristics of the BL Lac Objects Mkn 501 and Mkn 421 as Measured with the HEGRA Stereoscopic System of Imaging Atmospheric Cherenkov Telescopes

**F.A. Aharonian, M. Hemberger, G. Hermann, W. Hofmann, J. Kettler, A. Kohnle A. Konopelko, H. Krawczynski, H. Lampeitl, G. Pühlhofer, H.J. Völk, for the HEGRA Collaboration**
*Max–Planck–Institut für Kernphysik, Saupfercheckweg 1, D–69117 Heidelberg, Germany*

### Abstract

The HEGRA system of Imaging Atmospheric Cherenkov Telescopes (IACTs) has been used since the beginning of 1997 for a comprehensive study of the gamma-ray emission from the BL Lac objects Mkn 501 and Mkn 421 in the energy range above 500 GeV. Here we summarize the TeV characteristics of Mkn 501 during its spectacular outburst in 1997 and give an overview of the 1997 and 1998 Mkn 421 results.

## 1 Introduction

The two BL Lac sources Mkn 421 and Mkn 501 were the two first extragalactic sources established as TeV-emitters (Quinn et al. 1996; Bradbury et al. 1997; Punch et al. 1992; Petry et al. 1996) and have been subject to intense TeV studies ever since. The object Mkn 501, after showing moderate flux levels of one third the flux of the Crab Nebula during the first years after its discovery as a TeV $\gamma$-ray source, went during 1997 into a phase of surprisingly high activity and dramatic variability, outshining during several nights the brightest known source in the TeV sky, the Crab Nebula, by factors as large as $\sim 10$. The high activity allowed us to study the temporal characteristics of the source on time scales of several minutes and to perform detailed spectral studies on diurnal basis. In this contribution we summarize the results of the stereoscopic IACT system of HEGRA concerning the 1997 Mkn 501 emission and the 1997 and 1998 Mkn 421 radiation. We compare the TeV characteristics of the two sources and discuss the implications of the results on the density of the infrared Diffuse Extragalactic Background Radiation (DEBRA). Detailed further information on the Mkn 501 and Mkn 421 observations as well as on the analysis tools can be found in (Aharonian et al. 1999a–c, called A99a, A99b, and A99c in the following).

## 2 The IACT System of HEGRA, Data Sample, and Analysis Methods

The HEGRA system (Daum et al. 1997) of five (until fall 1998 four) IACTs is located on the Roque de los Muchachos on the Canary Island of La Palma, (lat. 28.8° N,long. 17.9°, 2200 m a.s.l.). Each telescope is equipped with a segmented 8.5 m$^2$ mirror and a 4.3° field of view high resolution camera consisting of 271 pixels of 0.25° diameter. Exploiting the stereoscopic observation technique (simultaneous observation of air showers under widely differing viewing angles with two or more Cherenkov telescopes), the system achieves an energy threshold of 500 GeV, an angular resolution of 0.1° and an energy resolution of better than 20% per individual photon, and an energy flux sensitivity $\nu F_\nu$ at 1 TeV of $10^{-11}\,\mathrm{ergs/cm^2 sec} \simeq$ 1/4 Crab for one hour of observation time (S/N=5$\sigma$).

The Mkn 501 analysis is based on 110 hours of observations acquired between March 16th, 1997 and October 1st, 1997. The Mkn 421 analysis is based on 165 hours of observations acquired between January 1st, 1997 and May 27th, 1998. Only data taken under optimal weather conditions, with the optimal detector performance, and with the source being more than 45° above the horizon were used for the analysis. Most of the analysis presented below use only the data with zenith angles up to 30°. The analysis tools as well as our methods to determine the systematic error on spectral estimates are described in (A99a; A99b). For minimizing the systematic uncertainties in the energy dependent cut-efficiencies, the analysis uses “loose” $\gamma$/hadron-separation cuts which accept a large fraction of $\sim 80\%$ of the $\gamma$-rays at all energies above 1 TeV. The analysis, i.e. the cut optimization and the calculation of effective detection areas and cut efficiencies, is based on detailed Monte

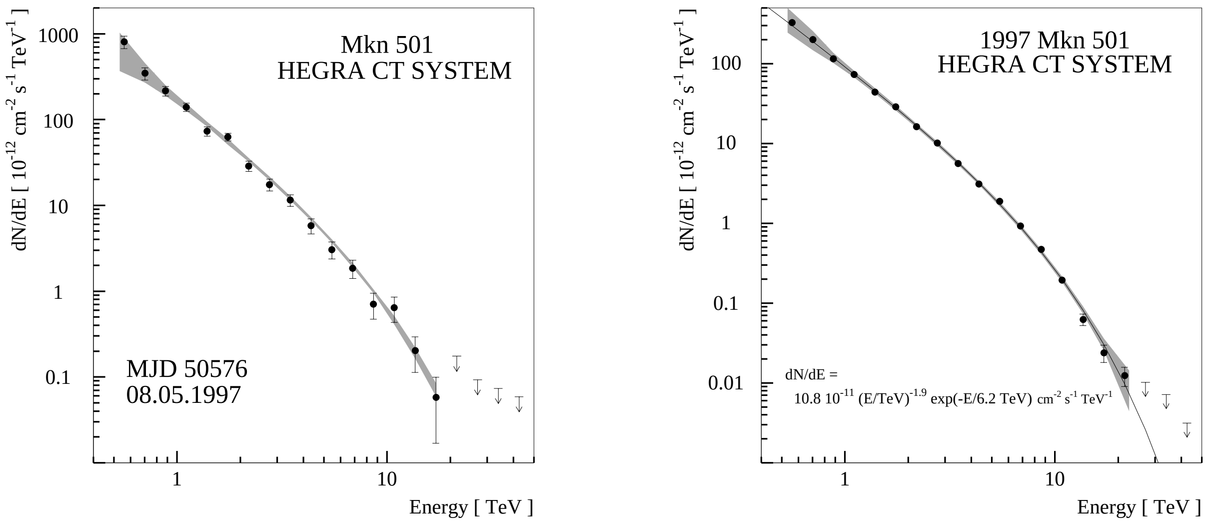


Figure 1: The left side shows a diurnal Mkn 501 energy spectrum taken with an integration time of 1.9 hours (data with $<30°$ zenith angle). The right side shows the 1997 time averaged Mkn 501 spectrum. (Upper limits are $2\sigma$ confidence level; vertical error bars show the statistical errors; the hatched region shows the systematic error on the curvature of the spectrum.)

Carlo simulations (Konopelko et al. 1998). Extensive studies, possible due to redundant shower information provided by an IACT system operated in the stereoscopic mode, were performed to reduce and to estimate the systematic error of the determined TeV energy spectra. The pointing accuracy of the IACTs was checked by verifying the Mkn 501 location to an accuracy of 35 arcsec (Pühlhofer et al. 1997).

# 3 Mkn 501 Results from 1997

For fluxes comparable to the Crab flux the stereoscopic IACT system of HEGRA has the sensitivity not only to assess within a fraction of an hour the TeV flux, but also to determine differential energy spectra on a diurnal basis. One of 63 diurnal Mkn 501 energy spectra obtained during the 1997 observation period is shown in Figure 1 (left side). The systematic error of the energy spectrum can be divided into two contributions: a 15% uncertainty on the absolute energy scale, and an error on the curvature of the spectrum, shown in the figure by the hatched region. It can be recognized that an integration time of 1.9 hours was sufficient to determine the differential spectrum over the broad energy region from 500 GeV to above 10 TeV, and to prove a significant deviation of the spectrum from a pure power law. The diurnal 1 TeV to 5 TeV photon index has been determined to be 2.24 with a statistical accuracy of 0.11 and a systematic accuracy of 0.05.

The 1997 light curve (see A99a) showed flux variations from a fraction of the Crab level to more than 10 Crab levels with flux increases/decreases by more than a factor of two within 24 hours. The 1 TeV to 5 TeV photon indices, determined with typical accuracies of between 0.1 and 0.3 remained surprisingly stable and no highly significant deviation from the mean index of 2.28 could be established. Furthermore, accumulating the data according to the diurnal 2 TeV flux levels, or according to a “rising” or “falling” flux behavior yielded time averaged spectra with the same curvature within statistical accuracies.

The 1997 time averaged Mkn 501 spectrum is shown in Figure 1 (right side). From 500 GeV to 24 TeV, the spectrum can be described by a power law model with an exponential cut off: $dN/dE = N_0\,(E/1\,\mathrm{TeV})^{-\alpha}\,\exp\left(-\mathrm{E}/\mathrm{E}_0\right)$, with $N_0 = (10.8 \pm 0.2_{\rm stat} \pm 2.1_{\rm syst}) \cdot 10^{-11}\,\mathrm{cm}^{-2}\mathrm{s}^{-1}\mathrm{TeV}^{-1}$, $\alpha = 1.92 \pm 0.03_{\rm stat} \pm 0.20_{\rm syst}$, and $E_0 = (6.2\ \pm 0.4_{\rm stat}\ (-1.5\ +2.9)_{\rm syst})$ TeV. The systematic errors on the fit parameters result from worst case assumptions concerning the systematic errors of the data points and their correlations, and include the error caused by the 15% uncertainty in the energy scale. Note that the error on $\mathrm{E}_0$ and $\alpha$ is strongly correlated. A dedicated $\chi^2$-analysis yields a very conservative lower limit on the maximum $\gamma$-ray energy in the signal of 16 TeV.

Intensive Mkn 501 multiwavelength campaigns have been performed with the aim to unambiguously iden-

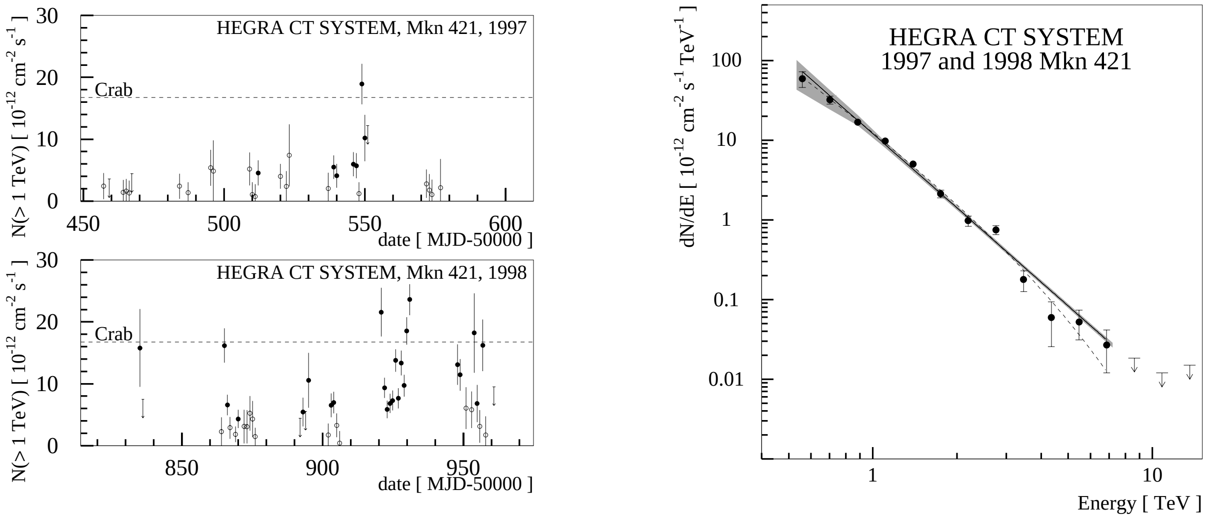


Figure 2: The left side shows the Mkn 421 lightcurve for 1997 and 1998. The right side shows the 1997–1998 time averaged Mkn 421 energy spectrum. The solid line shows the power law fit, the dashed line the fit of a power law with an exponential cutoff, both as described in the text. (Upper limits are $2\sigma$ confidence level; the error bars show the statistical errors; the hatched region show the systematic error on the curvature of the spectrum)

tify the emission mechanism. We found a significant correlation of the IACT system fluxes with the 2 keV-12 keV X-ray fluxes determined with the All Sky Monitor on board the RXTE *Rossi X-Ray Timing Explorer* (A99a). The analysis of multiwavelength campaigns performed during 1998 together with more sensitive pointed X-ray instruments with good spectroscopic capabilities, namely RXTE, and ASCA is underway.

## 4 Mkn 421 Results from 1997 and 1998

The 1997 and 1998 Mkn 421 lightcurve is shown in Figure 2 (left side). During our observations, the source showed moderate flux levels at 1 TeV of approximately one third of the Crab flux. During sporadic flares, the flux increased up to a level of between one and two Crab units. Also in the case of Mkn 421 we do not find significant evidence for spectral variability, neither studying the diurnal spectra, nor by dividing the data in a 1997 and 1998 data sample or in a high- and a low-flux data sample. A pure power law model satisfactorily describes the data over the energy range from 500 GeV to several TeV (Figure 2, right side, solid line): $d\mathrm{N}/d\mathrm{E} = \ (12.1\ \pm 0.5_{\rm stat}\ \pm 4.3_{\rm syst})\ 10^{-12}\,(\mathrm{E/TeV})^{(-3.09\,\pm 0.07_{\rm stat}\,\pm 0.10_{\rm syst})}\mathrm{cm}^{-2}\mathrm{s}^{-1}\mathrm{TeV}^{-1}$. Note that a power law with an exponential cutoff also fits the data (see Figure 2, right side, dashed line): $d\mathrm{N}/d\mathrm{E} \propto (\mathrm{E/TeV})^{(-2.5\pm 0.4_{\rm stat})}\exp(-\mathrm{E}/\mathrm{E}_0)$ with $\mathrm{E}_0 = 2.8\left(^{+2.0}_{-0.9}\right)_{\rm stat}$ TeV.

For the 1997 data we obtain a power law photon index of $3.28\ \pm 0.20_{\rm stat}$, for the 1998 data we get $3.00\ \pm 0.05_{\rm stat}$, and from the April 1998 data which was taken in the frame of a worldwide multiwavelength campaign (Takahashi et al. 1999), we obtain the photon index $3.03\ \pm 0.08_{\rm stat}$.

## 5 Discussion

The IACT system of HEGRA has been used to obtain a wealth of detailed spectral and temporal information about the TeV-emission of the two BL-Lac objects Mkn 501 and Mkn 421. For both sources, we studied the spectra on diurnal basis but did not find strong evidence neither for spectral variability nor for a correlation of absolute flux and spectral shape. In the case of Mkn 501, the high emission levels allowed us to assess the spectrum up to energies of $\simeq$20 TeV. The spectrum is well described by a power law with an exponential cutoff at 6.2 TeV. This cutoff could certainly be caused by several effects: it could reflect the maximum energy to which nonthermal particles are accelerated, it could show the increasing importance of TeV-photons being produced in Klein-Nishina Inverse Compton processes for increasing energies, it could be caused by absorption of the TeV-photons in pair production processes inside the source, or by extinction of the TeV photons by the

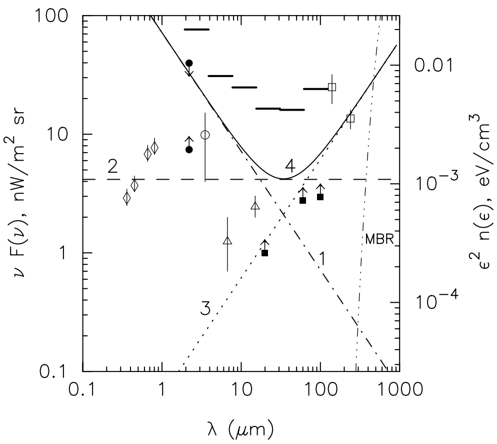


Figure 3: The figure shows estimates of the DEBRA energy flux $\epsilon^2\, n(\epsilon)$ by other experiments and constraints derived from the HEGRA observations. The horizontal bars show the DEBRA upper limit derived from the condition of a constant or increasing photon index of the TeV energy spectrum for increasing energy. Curve 1 shows $n(\epsilon)\ \propto\ \epsilon^{-1}$, normalized to yield a optical depth equal three. Curve 2 shows $n(\epsilon)\ \propto\ \epsilon^{-2}$, normalized to yield a TeV extinction for which the intrinsic Mkn 501 TeV spectrum would be a pure power law. Curve 3 shows $n(\epsilon)\ \propto\ \epsilon^{-3}$, normalized to yield as little as possible TeV extinction while being consistent with the COBE measurements of the DIRBE at 140 and 240 microns. A Hubble constant of 60 km/s Mpc has been assumed for our limits. The other measured fluxes and the upper/lower limit estimates of the DEBRA are taken from the recent compilation by Dwek et al. (1998). The curve marked as “MBR” shows to the density of the 2.7 K MBR.

DEBRA. As pointed out already in (A99a), the rather stable TeV spectra indicate a time independent spectrum of accelerated nonthermal particles together with cooling times of the very energetic particles which are too short to yield spectral cooling observable with the typical HEGRA integration times in the order of hours. Since Mkn 501 and Mkn 421 are located at similar redshifts (0.034 and 0.031, respectively), the DEBRA extinction would deform the Mkn 501 and the Mkn 421 spectra in the same way. Due to the low flux levels during our Mkn 421 observations we cannot verify or exclude at this time that the Mkn 421 spectrum cuts off at a similar energy as the Mkn 501 spectrum.

Under rather general assumptions the pure fact of recording Mkn 501 photons with energies well above 10 TeV yields sensitive upper limits on the DEBRA density in the wavelength region from 1 to 50 microns. Recent DEBRA estimates as well as constraints from the TeV-observations are shown in Figure 3. The requirement of a constant or increasing photon index for increasing TeV energies yields the upper limits shown by the horizontal bars. The requirement of an optical depth below 3, which would mean a TeV absorption by a factor of 20 (already very problematic for most emission models) yields an estimate of a maximum DEBRA density shown by curve 1. The latter DEBRA density could be reconciled with the positive DEBRA detections by COBE at 140 and 240 microns as shown by curve 3 and 4. Both arguments limit the DEBRA energy density to values about 10 nW/m$^2$ sr. Note that a constant DEBRA energy density per logarithmic bandwidth (curve 2) would deform a power law of photon index 1.92 exactly into the observed power law spectrum with an exponential cutoff at 6.2 TeV.


*Acknowledgments*
We thank the Instituto de Astrofísica de Canarias (IAC) for supplying excellent working conditions at La Palma. HEGRA is supported by the BMBF (Germany) and CYCIT (Spain).


# 6 References:


Aharonian F.A., Akhperjanian A.G., Barrio J.A., et al., 1999a, A&A 342, 69
Aharonian F.A., Akhperjanian A.G., Barrio J.A., et al., 1999b, submitted to A&A, astro-ph/9903386
Aharonian F.A., Akhperjanian A.G., Andronache M., et al., 1999c, submitted to A&A, astro-ph/9905032
Bradbury S.M., Deckers T., Petry D., et al., 1997, A&A 320, L5
Daum A., Hermann G., Heß M., et al., 1997, Astropart. Phys. 8, 1
Dwek E., Arendt R.G., Hauser et al., 1998, Ap.J. 508, 106
Konopelko A., Hemberger M., Aharonian F.A., et al., 1999, Astropart. Phys. 10, 275-289
Petry D., Bradbury S.M., Konopelko A., et al., 1996, A&A 311, L13
Pühlhofer G., Daum A., Hermann G., et al., 1997, Astropart. Phys. 8, 101
Punch M., Akerlof C.W., Cawley M.F., et al., 1992, Nat 358, 477
Quinn J., Akerlof C.W., Biller S., et al., 1996, ApJ 456, L83
Takahashi T., Madejski G., Kubo H., 1999. In: Proc. the Veritas Workshop on the TeV Astrophysics of Extragalactic Objects, ed. Weekes T.C., Catanese M., Astroparticle Physics in press.